

# MAGNETIC FIELD MEASUREMENT FOR A THZ UNDULATOR USING THE VIBRATING WIRE METHOD

Shigeru Kashiwagi<sup>#</sup>, Yuu Tanaka, Fujio Hinode, Masayuki Kawai, Xiangkun Li,  
Toshiya Muto, Ken-ichi Nanbu, Hiroyuki Hama  
Electron Light Science Centre, Tohoku University, Sendai, Miyagi 982-0826, Japan

## Abstract

We constructed an undulator of Halbach planer type for generation of intense coherent terahertz radiation (THz) with the very short electron bunch. The length and the number of periods are 100 mm and 25, respectively. Its maximum magnetic field is 0.41 T and K-value is 3.82 with 54 mm gap. The vibrating wire method is studied to measure the magnetic field of the undulator. The numerical studies have been performed for the THz undulator and derived a relation between a reproducibility of undulator field and the number of the harmonic modes [1]. A test experiment was carried out using 200 mm wire and a pair of permanent magnet blocks. The results of the test experiment are described.

## INTRODUCTION

A test accelerator for a terahertz source project (t-ACTS) has been progressed at the Electron Light Science Centre, Tohoku University, in which generation of intense coherent terahertz radiation from the very short electron bunch will be demonstrated [2]. A narrow-band coherent terahertz radiation with an undulator has been considered to be implemented in the t-ACTS project. The planar undulator of Halbach type had been developed for the coherent terahertz radiation. This undulator produces the terahertz radiation and its wavelength is 360~170  $\mu\text{m}$  (0.8~1.7 THz) with 17 MeV electron beam [2].

The synchrotron radiation from the electron beam passing through an undulator can be estimated using a magnetic field distribution in an undulator. Therefore, it is important to measure and characterize the magnetic field of an undulator precisely. Also in manufacture, a precise magnetic field measurement is indispensable in order to achieve high magnetic performances (uniformity etc.).

Magnetic field measurement using a Hall probe is used widely in undulator development. Magnetic field of the THz undulator was also measured by Hall probes in the manufacturing company. However, the measurement system is large and expensive, and may not be easily available in our laboratory. Therefore, we started to study and develop a suitable measurement method for the THz undulator. We chose the vibrating wire method to measure magnetic field of the THz undulator. The vibrating wire method [3] does not require special equipment, because this method only uses a stretched wire as a magnetic probe, the apparatus can be simple. This method can measure the periodic undulator field and we can find a local magnetic error by comparing with ideal magnetic field distribution. In a case of undulator with large

number of periods or short period length, number of modes to be measured is increased and the vibration frequency becomes high. Therefore, this vibrating wire method is unsuitable for an undulator with large number of periods or short period length. Conversely, the vibrating wire method suits to measure the undulator having a small number of periods and a long period length as our THz undulator.

## VIBRATING WIRE METHOD

The vibrating wire method employs a wire stretched through the measured magnetic field. The Lorentz forces between AC current flowing to the wire and given magnetic field cause the wire vibration. The resonant standing-wave mode is excited at each eigenmode frequencies. By measuring the amplitude of the resonance modes, harmonic mode of the magnetic field distribution can be obtained. The undulator field can be reconstructed by means of the inverse Fourier transformation.

The equation of motion ( $U(z, t)$ ) for the wire in vertical direction can be described as

$$\mu \frac{\partial^2 U}{\partial t^2} + \gamma \frac{\partial U}{\partial t} - T \frac{\partial^2 U}{\partial z^2} = -\mu g + I(t)B(z) \quad (1)$$

where the  $\mu$ ,  $\gamma$  and  $T$  are a line density, damping constant and tension of wire, respectively. The first driving term due to gravity is time independent. The second driving term due to the AC current interacting with magnetic field is dynamical term and the current in wire may be presented as  $I(t) = I_0 e^{i\omega t}$ . A general solution to the differential equation can be given by the sum of particular solutions:  $U(z, t) = U_G(z) + U_D(z, t)$ . The dynamical term  $U_D(z, t)$  is represented by Fourier sine series  $U_B(z)$ ,

$$U_D(z, t) = U_B(z) \cdot \exp(i\omega t), \quad (2)$$

$$U_B(z) = \sum_{n=1}^{\infty} U_n \sin(n\pi z/L). \quad (3)$$

$U_n$  is the n-th order Fourier coefficient. The magnetic field  $B(z)$  may be represented in the same way:

$$B(z) = \sum_{n=1}^{\infty} B_n \sin(n\pi z/L) \quad (4)$$

From these equations we get a relation between  $U_D$  and  $B_n$

$$U_D(z, t) = \sum_{n=1}^{\infty} \frac{B_n \sin(n\pi z/L)}{\mu(\omega^2 - \omega_n^2 + i\gamma\omega)} \cdot I_0 \cdot e^{i\omega t} \quad (5)$$

where  $\omega_n$  is the resonance frequency of the n-th mode. By measuring the amplitude of wire vibration, we can get the Fourier coefficient of vibration  $U_n$  and can derive the

<sup>#</sup>kashiwagi@lms.tohoku.ac.jp

Fourier coefficient of magnetic field distribution  $B_n$ . The relation between  $U_n$  and  $B_n$  is  $U_n = (I_0 / \mu\gamma\omega_n) B_n$  at resonance.

*Finding Magnet Blocks with Strength Error*

In this section, we perform a numerical study to find a pathological magnetic block by the vibrating wire method. Setup of this study is same as Ref. 1. It is assumed that a magnet block with a strength error is contained in the magnet array of the THz undulator. The strength of the magnet block (Br) is 1% larger than that of others and the position of the magnet is set to 10<sup>th</sup> pole from upstream (vertical magnetized block). The strength of maximum field and error field are approximately 4100 Gauss and 7 Gauss, respectively. The magnetic field with the error is shown in Fig. 1(a) and the beam trajectory is deflected by the error field as shown in Fig. 1(c).

We calculate the Fourier coefficient of magnetic field  $B_n$  from the field given as Fig. 1(a). The error component is obtained by summing modes up to 10<sup>th</sup>, 20<sup>th</sup>, and 30<sup>th</sup> using Eq. (4). The reconstructed error field is compared with the design field reconstructed in the same way. The

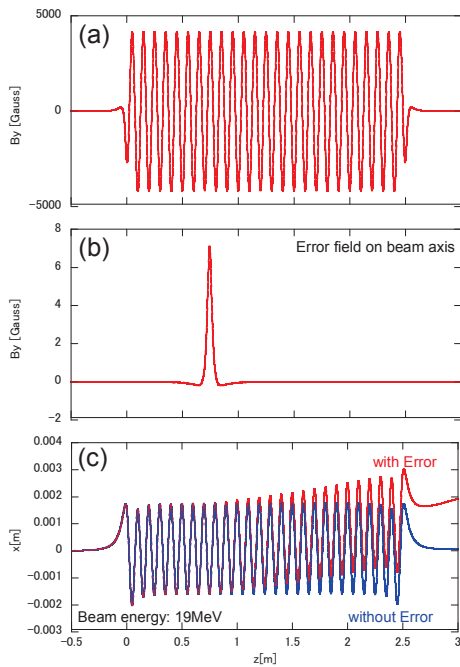


Figure 1: (a) Magnetic field distribution of the undulator with the error magnet. (b) Magnetic field by the error magnet block at  $z=0.75\text{m}$ . (c) Electron trajectory with and without error magnet block. ( $E = 19\text{MeV}$ )

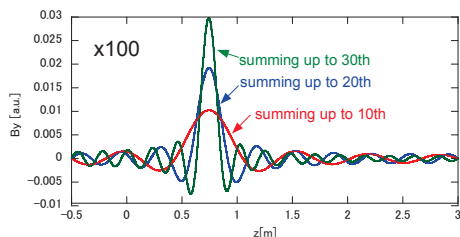


Figure 2: Reconstructed distribution of error magnetic field. (The vertical axis is magnified 100 times).

differences are represented in Fig. 2. In the Ref. 1, we pointed out that it was necessary to measure modes up to the 135<sup>th</sup> to reproduce the undulator field with a better resolution than distortion by geomagnetism. According to Fig.2, it is sufficient to measure modes up to 20<sup>th</sup> in order to identify the magnet block with strength error.

**TEST EXPERIMENT USING VIBRATING WIRE METHOD**

*Experimental Setup*

We carried out a test experiment by using a copper-beryllium wire with 200  $\mu\text{m}$  diameter and 200 mm length. Both ends of the wire were supported by ceramic bridges as shown in Fig. 3. A weight to fix the wire was 2.2 kg and the fundamental resonant frequency of the vibrating wire is 719.9 Hz ( $\mu = 2.6 \times 10^{-4} \text{ kg/m}$ ). A sensor to measure the wire vibration was the laser sensor (Keyence, LK-H020 and LK-G5000V), which was set to 20 mm from a support point. AC current is applied from one end of the wire and is terminated with 50 Ohm at another end. The AC current was monitored with a toroidal current transformer (CT).

*Data Acquisition System*

Configuration of data acquisition system is shown in Fig. 4. The analog signal from the laser sensor, AC current signal measured by CT and a synchronous signal from a function generator are simultaneously recorded by a sampling digitizer of PXI system. Since the analog signal includes noise of high frequency component, thus the noise is removed using FFT processing. The wire vibration amplitude was measured as a function of the frequency of AC current as shown in Fig. 5. The

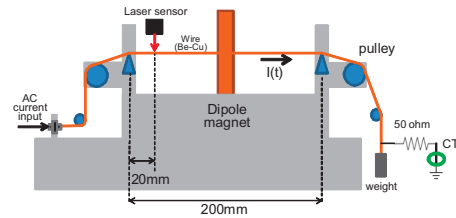


Figure 3: Setup of the test experiment for the vibrating wire method.

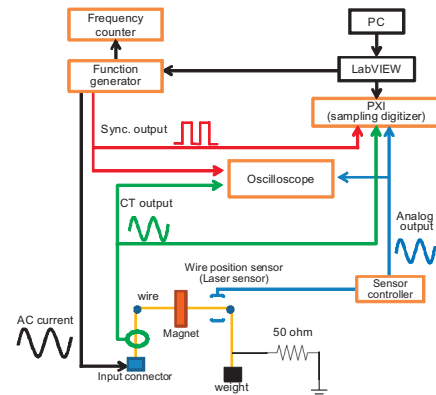


Figure 4: Configuration of data acquisition system.

amplitude of the wire vibration was analyzed by fitting with formula

$$U_n(\omega) = \frac{a_n}{\sqrt{(\omega^2 - b_n^2)^2 + (\omega c_n)^2}} \quad (6)$$

where  $a_n$ ,  $b_n$  and  $c_n$  are fitting parameters. The Fourier component  $B_n$  is obtained from  $a_n$  as

$$B_n = \langle a_n \rangle \frac{1}{\sin(\pi n z_s / L)} \frac{\mu}{I_0} \quad (7)$$

where  $\langle a_n \rangle$  means the average of  $a_n$  and the  $z_s$  is a sensor position. The measurement error of  $B_n$  is given by  $\sigma_{B_n} = (\partial B_n / \partial a_n) \sigma_a$ .

### Measurement Results

We measured magnetic field distribution using a Hall probe for comparison. We measured the wire vibration up to 25th harmonics and derived the Fourier coefficients ( $B_n$ ). In the measurement using Hall probe, the measured magnetic field expanded into Fourier series. Fig. 6 shows the absolute values of the Fourier coefficient as a function of mode number. The even-mode was approximately zero and any modes on the vibration wire were not excited, since the magnet was placed in the center of the wire. In the low frequency modes, the Fourier coefficients of two measurements were in agreement. We reconstructed the magnetic field distribution by the inverse Fourier transformation. The reconstructed field distributions summing modes up to 10<sup>th</sup>, 15<sup>th</sup>, 20<sup>th</sup> and 25<sup>th</sup> are shown in Fig. 7. The red dots and blue line represent the result of the vibrating wire and Hall probe measurements, respectively. The peak magnetic fields in the both measurements agreed with less than 5%. At the both sides of peak magnetic field in Fig. 7, the strength and

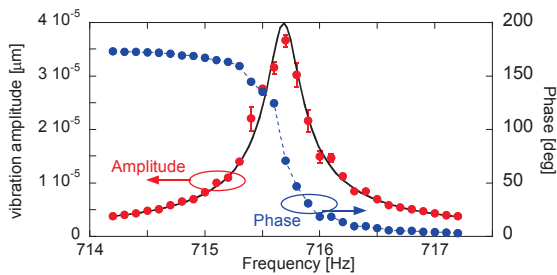


Figure 5: Example of amplitude and phase of wire vibration as function of the frequency of the driving current at the fundamental mode.

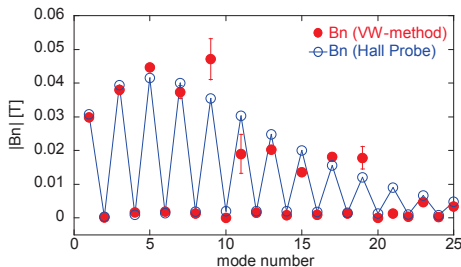


Figure 6: The Fourier coefficient of magnetic field. (1st ~25th harmonics) measured by the vibrating wire method and hall probe.

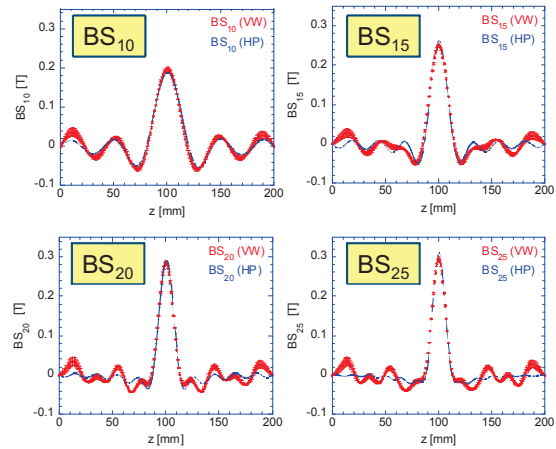


Figure 7: The reconstructed magnetic field  $BS_m(z)$  using modes up to 10(upper-left), 15(upper-right), 20(bottom-left) and 25 (bottom-right).

periodicity of reconstructed field were different. These differences can be caused by the measurement error of the vibration amplitude in higher modes. As shown in Fig. 6, the measured  $B_n$  for 9<sup>th</sup> and 11<sup>th</sup>, 19<sup>th</sup> and 21<sup>st</sup> modes were largely different for the two methods and the error bar of the vibrating wire method for the four modes were large comparing with other modes. The reason is that the vibrating amplitudes become very small in these modes, because the position of the laser sensor is close to a node of the vibration. To improve a resolution of measurement, we propose to optimize the sensor position for each mode.

### SUMMARY

We have numerically examined to find the error magnet block in the THz undulator by using the vibrating wire method. In order to find the error magnet block, we don't need to measure the many modes as mentioned in Ref. 1. It will be sufficient to measure modes up to 20<sup>th</sup>.

The test experiment has been performed using a set of dipole magnet block. Depending on the mode, the vibration amplitude was extremely small and it was difficult to measure. Therefore the position of the laser sensor for wire vibration should be changed in each mode to improve the accuracy of measurement.

### ACKNOWLEDGMENT

This work is supported by the Ministry of Education, Science, Sports and Culture, Grant-in-Aid for Scientific Research (S), Contract #20226003.

### REFERENCES

- [1] Y. Tanaka et al., Proc of FEL 2011, Shanghai (2011)
- [2] H. Hama et al., Nucl Instr. and Meth., A637 (2011) S57-S61, F. Hinode et al., Nucl Instr. and Meth., A637 (2011) S72-S75
- [3] A. Temnykh et al., Nucl. Inst. and Meth, A399 (1997) 185-194., A. Temnykh et al., Nucl. Instr. and Meth., A515 (2003) 387-393., A. Temnykh et al., Nucl. Instr. and Meth., A622 (2010) 650-656.